Calculation of Franck–Condon factors including anharmonicity: Simulation of the $C_2H_4^+ \tilde{X}\,^2B_{3u} \leftarrow C_2H_4 \tilde{X}\,^1A_g$ band in the photoelectron spectrum of ethylene

Josep M. Luis,[a] Miquel Torrent-Sucarrat, and Miquel Solà
Institute of Computational Chemistry and Department of Chemistry, University of Girona, Campus de Montilivi, 17071 Girona, Catalonia, Spain

David M. Bishop
Department of Chemistry, University of Ottawa, Ottawa K1N 6N5, Canada

Bernard Kirtman
Department of Chemistry and Biochemistry, University of California, Santa Barbara, California 93106

Our new simple method for calculating accurate Franck–Condon factors including nondiagonal (i.e., mode-mode) anharmonic coupling is used to simulate the $C_2H_4^+ \tilde{X}\,^2B_{3u} \leftarrow C_2H_4 \tilde{X}\,^1A_g$ band in the photoelectron spectrum. An improved vibrational basis set truncation algorithm, which permits very efficient computations, is employed. Because the torsional mode is highly anharmonic it is separated from the other modes and treated exactly. All other modes are treated through the second-order perturbation theory. The perturbation-theory corrections are significant and lead to a good agreement with experiment, although the separability assumption for torsion causes the C_2D_4 results to be not as good as those for C_2H_4. A variational formulation to overcome this circumstance, and deal with large anharmonicities in general, is suggested. © *2005 American Institute of Physics.*
[DOI: 10.1063/1.1896362]

I. INTRODUCTION

The role of *ab initio* calculations in the assignment of experimental high-resolution vibronic spectra has been drawing increased attention. Within the Born–Oppenheimer approximation, the leading term of the expansion that governs the spectral intensity is given by the square of the vibrational overlap integral ($|\langle \psi_{v_g}^g | \psi_{v_e}^e \rangle|^2$), also known as the Franck–Condon factor[1,2] (FCF), between the initial ($\psi_{v_g}^g$) and final states ($\psi_{v_e}^e$). When the initial vibrational state is totally symmetric, only a totally symmetric vibrational final state (referring to the largest common point subgroup) will have a nonzero FCF. There are, of course, smaller contributions to the intensity due to higher-order terms in the expansion, governed by Herzberg–Teller factors,[3] but we will focus on FCFs in this paper.

Since the equilibrium geometry and potential-energy surface (PES) of the initial and final electronic states are different the $3N$-6 (or $3N$-5 for linear molecules) dimensional FCF overlap integrals cannot be factored into a simple product of one-dimensional normal-mode integrals. A wide variety of methods, based on the harmonic approximation for the PES of both the initial and final states, has been presented to solve this problem. One such method is the generating function approach of Sharp and Rosenstock,[4] which has been further developed by Chen,[5] and later improved by Ervin *et al.*[6] A simpler form of the Sharp and Rosenstock's general formula

was recently derived by Kikuchi *et al.*[7] The most popular alternative to the generating function approach utilizes the recursion relations of Doctorov *et al.*[8] Segev and co-workers[9,10] have developed another interesting alternative from a completely different point of view that relies on the consideration of the transitions in phase space.

Including vibrational anharmonicity always implies a strong increase in computational cost and, for most methods, the formulation becomes much more complex as well. That explains why the papers mentioned above did not consider vibrational anharmonicity. On the contrary, there have been several attempts to take anharmonicity into account, at least partially. The procedures of Iachello and co-workers[11,12] are based on a novel Lie algebraic scheme that employs Morse oscillators. Mok *et al.*[13] use anharmonic vibrational wave functions expressed as a linear combination of harmonic-oscillator functions together with the complete Watson Hamiltonian. This method, seemingly limited in practice to small molecules, has recently been employed by Mok and co-workers to calculate FCFs for absorption spectra of several triatomic molecules.[14–17] Very recently Hazra *et al.*[18] presented the so-called vertical Franck–Condon approach, in which the final state PES is expanded around the equilibrium geometry of the initial state. They assume separability of the normal modes and, if the curvature in the final state is negative, they incorporate the full one-dimensional (1D) potential. In applying this method to simulate the ultraviolet spectrum of ethylene, for example, a full 1D potential was used for torsion along with a pure harmonic potential for the remaining $3N$-7 modes. In this paper we also use a full 1D

---
[a]Author to whom correspondence should be addressed. Electronic mail: josepm.luis@udg.es

potential for the torsion mode of ethylene, but separability is not assumed for the remaining $3N$-7 modes. To our knowledge there are no other calculations for a molecule with more than three atoms that have included nondiagonal anharmonic coupling.

Recently we presented a simple new procedure to evaluate FCFs which, among other things, can account for nondiagonal anharmonic coupling.[19] In the present study we apply our method to the $C_2H_4^+\tilde{X}\,^2B_{3u}\leftarrow C_2H_4\tilde{X}\,^1A_g$ band in the photoelectron spectrum including Duschinsky[20] rotations and anharmonic effects in calculating the Franck–Condon factors. Both the hydrogenic and the fully deuterated species are examined. In this application an important consideration is the geometry of the radical cation. Whereas the experimental ground state of neutral ethylene is planar,[21] the ground state of the radical cation has a twisted D_2 equilibrium geometry, as deduced from the vacuum ultraviolet spectrum observed by Merer and Schoonveld.[22] Subsequent photoelectron spectroscopy, which permits direct investigation of the cation, showed an extended progression in the torsional mode, thereby providing further evidence for the twisted geometry.[23,24] Pollard *et al.*[23] analyzed this progression to obtain an equilibrium dihedral angle of $27°\pm2°$ and a torsion barrier of 270 ± 150 cm^{-1}. Recently, Willitsch *et al.*[25] recorded pulsed-field-ionization zero-kinetic-energy (PFI-ZEKE) photoelectron spectra of $C_2H_4^+$ and $C_2D_4^+$ with a resolution that is two to three orders of magnitude greater than classical photoelectron spectra. These new accurate data give a torsional barrier of 357 ± 26 (292 ± 24) cm^{-1} along with a dihedral angle of $29.2°\pm0.5°$ ($27.8°\pm0.5°$) for $C_2H_4^+$ ($C_2D_4^+$). The ground and first excited torsional states were found to lie below the barrier at the planar geometry. They constitute a tunneling pair with a splitting of 83.7 (37.1) cm^{-1} for $C_2H_4^+$ ($C_2D_4^+$). Given the low torsional barrier the molecular symmetry of the ethylene cation may be regarded as effectively D_{2h} rather than D_2.[25] This effective symmetry is consistent with the fact that even peaks of the progression in the torsional mode are far more intense than the odd peaks.

The purpose of this study is to simulate the $C_2H_4^+\tilde{X}\,^2B_{3u}\leftarrow C_2H_4\tilde{X}\,^1A_g$ spectrum and, by the same token, demonstrate the feasibility of our recently published procedure[19] for evaluating FCFs of a polyatomic molecule with anharmonicity and Duschinsky rotations fully taken into account. In Sec. II a summary of our general formulation for calculating FCFs is presented. Then, in Sec. III we give specific computational details regarding simulation of the He I photoelectron (PE) spectrum of C_2H_4 and C_2D_4. This is followed by a discussion of our results and, finally, some concluding remarks and future plans.

II. THEORY

Recently several of us presented a new analytical procedure for calculating Franck–Condon factors of polyatomic molecules taking into account both the Duschinsky rotations and anharmonicity.[19] In this section we summarize the most important relations of our new methodology.

A. General simultaneous equations for Franck–Condon factors

Our starting point is the Schrödinger equation for nuclear motion in the ground and excited electronic states. Assuming a nonrotating molecule, and taking advantage of the Hermitian property of the vibrational Hamiltonian, one can readily obtain[19]

$$\langle \psi^g_{v_g}|\hat{H}^g-\hat{H}^e|\psi^e_{v_e}\rangle = (E^g_{v_g}-E^e_{v_e})S_{v_g v_e}. \tag{1}$$

In Eq. (1) $\hat{H}^g$, $|\psi^g_{v_g}\rangle$, and $E^g_{v_g}$ are the vibrational Hamiltonian, wave function, and energy of the ground electronic state; $\hat{H}^e$, $|\psi^e_{v_e}\rangle$, and $E^e_{v_e}$ are their counterparts for the electronic excited state; and $S_{v_e v_g}$ is a Franck–Condon overlap integral,

$$S_{v_e v_g} = S_{v_g v_e} = \langle \psi^e_{v_e}|\psi^g_{v_g}\rangle = \langle \psi^g_{v_g}|\psi^e_{v_e}\rangle. \tag{2}$$

Since the vibrational eigenfunctions for the excited electronic state form a complete set ($\psi^e_{\mu_e}$ below) the left-hand side (lhs) of Eq. (1) can be expressed as

$$\langle \psi^g_{v_g}|\hat{H}^g-\hat{H}^e|\psi^e_{v_e}\rangle = \sum_{\mu_e}\langle \psi^g_{v_g}|\psi^e_{\mu_e}\rangle\langle \psi^e_{\mu_e}|\hat{H}^g-\hat{H}^e|\psi^e_{v_e}\rangle$$

$$= \sum_{\mu_e} S_{v_g \mu_e}\langle \psi^e_{\mu_e}|\hat{H}^g-\hat{H}^e|\psi^e_{v_e}\rangle. \tag{3}$$

Then, using the fact that the total nuclear kinetic-energy operator is the same for $\hat{H}^g$ and $\hat{H}^e$, one can combine Eqs. (1) and (3) to obtain a set of homogeneous linear simultaneous equations for a given v_g,

$$\sum_{\mu_e} S_{v_g \mu_e}[\langle \psi^e_{\mu_e}|\hat{V}^g-\hat{V}^e|\psi^e_{v_e}\rangle + (E^e_{v_e}-E^g_{v_g})\delta_{\mu_e v_e}] = 0, \quad \forall\, v_e, \tag{4}$$

in which $\delta_{\mu_e v_e}$ is the Kronecker delta. In practice this infinite set of equations must be truncated. A systematic and efficient iterative algorithm for selecting the M equations that survive the truncation is given in Sec. II D. After dividing each term in Eq. (4) by $S_{v_g \lambda_e}$ (λ_e is arbitrary as long as $S_{v_g \lambda_e}\neq 0$) we have

$$\sum_{\mu_e}^{M} r^{\mu_e}_{\lambda_e}[\langle \psi^e_{\mu_e}|\hat{V}^g-\hat{V}^e|\psi^e_{v_e}\rangle + (E^e_{v_e}-E^g_{v_g})\delta_{\mu_e v_e}] = 0$$

$$\{v_e\} = \{\mu_e\}, \quad \forall\, v_e, \tag{5}$$

where

$$r^{\mu_e}_{\lambda_e} = S_{v_g \mu_e}/S_{v_g \lambda_e}, \tag{6}$$

and the index v_g is suppressed in the symbol for this ratio. Because the simultaneous equations are homogeneous there is a redundancy and it is convenient to obtain a solution by

means of singular value decomposition. Once the ratios have been determined, the Franck–Condon overlap integrals can be obtained from the normalization condition,

$$S_{v_g\mu_e} = \frac{r_{\lambda_e}^{\mu_e}}{\sqrt{\sum_{\mu_e}^{M} (r_{\lambda_e}^{\mu_e})^2}}. \tag{7}$$

Finally, the Franck–Condon factors are just the square of the corresponding Franck–Condon integrals, i.e., $F_{v_g\mu_e} = S_{v_g\mu_e}^2$.

B. Duschinsky rotations

The normal coordinates of the electronic excited and ground states ($\mathbf{Q^e}$ and $\mathbf{Q^g}$) are different. They are related by the equation,[19]

$$\mathbf{Q^g} = \mathbf{JQ^e} + \mathbf{K}, \tag{8}$$

where $\mathbf{J}$ is the Duschinsky rotation matrix and $\mathbf{K}$ is a vector associated with the change in equilibrium geometry between the two electronic states. $\mathbf{J}$ and $\mathbf{K}$, in turn, may be written in terms of the unitary matrices that transform the mass-weighted Cartesian displacement coordinates to normal coordinates[26] (i.e., $\mathbf{Q^g} = \mathbf{L^{g\dagger}X^g}$ and $\mathbf{Q^e} = \mathbf{L^{e\dagger}X^e}$),

$$\mathbf{J} = \mathbf{L^{g\dagger}L^e} \quad \text{and} \quad \mathbf{K} = \mathbf{L^{g\dagger}R}. \tag{9}$$

In Eq. (9) $\mathbf{R}$ is the vector obtained by subtracting the ground-state equilibrium geometry from that of the excited state, both being expressed in terms of mass-weighted Cartesian coordinates. By taking advantage of Eq. (8), one can write the potential-energy difference $\hat{V}^g - \hat{V}^e$, that appears in Eq. (5), solely as a function of the excited electronic state normal coordinates. In the harmonic approximation,

$$\hat{V}^g - \hat{V}^e = V_{Q^g=0}^g - V_{Q^e=0}^e + \frac{1}{2}\sum_{i=1}^{3N-6}\left[\frac{\partial^2 V^g}{\partial(Q_i^g)^2}\right]_{Q^g=0}$$
$$\times\left[K_i^2 + 2K_i\sum_{j=1}^{3N-6}J_{ij}Q_j^e + \sum_{j,k=1}^{3N-6}J_{ij}J_{ik}Q_j^eQ_k^e\right]$$
$$-\frac{1}{2}\sum_{i=1}^{3N-6}\left[\frac{\partial^2 V^e}{\partial(Q_i^e)^2}\right]_{Q^e=0}(Q_i^e)^2. \tag{10}$$

C. Anharmonicity

The effect of anharmonicity can be accounted for by perturbation theory. We write the zeroth-order, i.e., harmonic, equation as

$$\sum_{\mu_e}^{M} S_{v_g\mu_e}^{(0)}\left[\langle\psi_{\mu_e}^e|\hat{V}^g-\hat{V}^e|\psi_{v_e}^e\rangle + (E_{v_e}^e - E_{v_g}^g)\delta_{\mu_e v_e}\right]^{(0)} = 0, \tag{11}$$

where

$$\langle\psi_{\mu_e}^e|\hat{V}^g-\hat{V}^e|\psi_{v_e}^e\rangle^{(0)} = \langle\psi_{\mu_e}^{e(0)}|(\hat{V}^g-\hat{V}^e)^{(0)}|\psi_{v_e}^{e(0)}\rangle, \tag{12}$$

and $(\hat{V}^g-\hat{V}^e)^{(0)}$ is given by the right-hand side of Eq. (10). If the cubic and quartic terms in $\hat{V}^g$ and $\hat{V}^e$ are defined to be

first and second order, respectively,[27] then the first-order perturbation equation is

$$\sum_{\mu_e} S_{v_g\mu_e}^{(1)}\left[\langle\psi_{\mu_e}^e|\hat{V}^g-\hat{V}^e|\psi_{v_e}^e\rangle + (E_{v_e}^e - E_{v_g}^g)\delta_{\mu_e v_e}\right]^{(0)}$$
$$+ \sum_{\mu_e} S_{v_g\mu_e}^{(0)}\left[\langle\psi_{\mu_e}^e|\hat{V}^g-\hat{V}^e|\psi_{v_e}^e\rangle + (E_{v_e}^e - E_{v_g}^g)\delta_{\mu_e v_e}\right]^{(1)} = 0, \tag{13}$$

in which

$$\langle\psi_{\mu_e}^e|\hat{V}^g-\hat{V}^e|\psi_{v_e}^e\rangle^{(1)} = \langle\psi_{\mu_e}^{e(1)}|(\hat{V}^g-\hat{V}^e)^{(0)}|\psi_{v_e}^{e(0)}\rangle$$
$$+ \langle\psi_{\mu_e}^{e(0)}|(\hat{V}^g-\hat{V}^e)^{(1)}|\psi_{v_e}^{e(0)}\rangle$$
$$+ \langle\psi_{\mu_e}^{e(0)}|(\hat{V}^g-\hat{V}^e)^{(0)}|\psi_{v_e}^{e(1)}\rangle, \tag{14}$$

$$|\psi_{v_e}^{e(1)}\rangle = -\sum_{\mu_e \neq v_e}^{M} \frac{\langle\psi_{v_e}^{e(0)}|\hat{V}^{e(1)}|\psi_{v_e}^{e(0)}\rangle|\psi_{\mu_e}^{e(0)}\rangle}{E_{\mu_e}^{e(0)} - E_{v_e}^{e(0)}}, \tag{15}$$

and

$$(\hat{V}^g - \hat{V}^e)^{(1)} = \frac{1}{6}\sum_{i,j,k=1}^{3N-6}\left(\frac{\partial^3 V^g}{\partial Q_i^g\partial Q_j^g\partial Q_k^g}\right)_{Q^g=0}$$
$$\times\left[K_iK_jK_k + 3K_iK_j\sum_{l=1}^{3N-6}J_{kl}Q_l^e + 3K_i\right.$$
$$\times\sum_{l,m=1}^{3N-6}J_{jl}J_{km}Q_l^eQ_m^e$$
$$\left.+ \sum_{l,m,n=1}^{3N-6}J_{il}J_{jm}J_{kn}Q_l^eQ_m^eQ_n^e\right]$$
$$-\frac{1}{6}\sum_{i,j,k=1}^{3N-6}\left(\frac{\partial^3 V^e}{\partial Q_i^e\partial Q_j^e\partial Q_k^e}\right)_{Q^e=0}Q_i^eQ_j^eQ_k^e, \tag{16}$$

while the first-order corrections to $E_{v_e}^e$ and $E_{v_g}^g$ vanish.[19] The column vector $\mathbf{S}_{vg}^{(1)}$ can be divided into a component orthogonal to $\mathbf{S}_{vg}^{(0)}$ (i.e., $\mathbf{S}_{vg}^{\prime(1)}$) plus a parallel component (i.e., $\mathbf{S}_{vg}^{\prime\prime(1)}$):

$$\mathbf{S}_{vg}^{(1)} = \mathbf{S}_{vg}^{\prime(1)} + \mathbf{S}_{vg}^{\prime\prime(1)} = \mathbf{S}_{vg}^{\prime(1)} + f\mathbf{S}_{vg}^{(0)}. \tag{17}$$

Evidently, the first term on the lhs of Eq. (13) vanishes regardless of the constant f in Eq. (17) [cf. Eq. (11)]. Hence, we are free to choose $f=0$ so that $\mathbf{S}_{vg}^{(1)}$ satisfies the first-order normalization condition,

$$\mathbf{S}_{vg}^{(1)\dagger}\mathbf{S}_{vg}^{(0)} = \mathbf{S}_{vg}^{\prime(1)\dagger}\mathbf{S}_{vg}^{(0)} = 0. \tag{18}$$

$\mathbf{S}_{vg}^{(1)}$ is most simply obtained by transforming Eq. (13) to a basis spanned by $\mathbf{S}_{vg}^{(0)}$ and an arbitrary set of $M-1$ vectors

perpendicular to $\mathbf{S}_{\mathbf{vg}}^{(0)}$. This leads to a set of $M-1$ inhomogeneous linear equations which are easily solved. Finally, the first-order corrections to the FCFs are

$$F_{v_g\mu_e}^{(1)} = 2S_{v_g\mu_e}^{(0)}S_{v_g\mu_e}^{(1)}. \tag{19}$$

A similar procedure may be followed for the second-order corrections.[19]

D. Truncation of the vibrational basis set

Perhaps the most critical step in our new procedure is the truncation of the vibrational basis set for the excited electronic state. This basis set must contain all functions necessary to obtain accurate FCFs, but must also be small enough for the calculations to be efficient. The algorithm we use involves an iterative buildup of the basis set by increasing the range of vibrational quantum numbers while, simultaneously, removing unnecessary functions. In the current work we have improved our previous truncation procedure so that rapid calculations including anharmonicity are possible for a molecule such as ethylene which contains 11 coupled normal modes.

The first step is to choose an initial reference vibrational state. One convenient option is to select the state determined by the Franck–Condon principle. In fact, it is not necessary to be very particular about this choice. Even the ground vibrational state is satisfactory except for spectra where the most intense peaks correspond to large vibrational quantum numbers. The selected reference state gives a starting vector of vibrational quantum numbers for all modes. A set of maximum quantum numbers for the initial iteration is obtained by adding unity to the starting values. Likewise a set of minimum quantum numbers is prepared by subtracting unity with the proviso that negative quantum numbers cannot occur. The initial trial basis set consists of all vibrational wave functions with quantum numbers in the range determined by the maximum and minimum values just described. There is one additional requirement that is enforced at the beginning of every iteration. It is based on the difference between the quantum numbers that characterize the vibrational state in question and those of the reference state. We compute the absolute value of the quantum number difference for each mode and, then, sum over all modes. If that sum is larger than a threshold value, the state is excluded from the basis set. The threshold value, in turn, is taken to be the largest difference between the maximum and minimum quantum numbers for any one mode which, in the first iteration, is either 1 or 2.

Given a trial basis, the associated set of FCFs is determined by solving the resulting linear simultaneous equations to the desired order of perturbation theory [e.g., Eqs. (11) plus (13) for the FCFs through first order]. All FCFs smaller than a certain threshold (we normally use 10^{-7}) are set equal to zero and the corresponding vibrational states are marked for exclusion in further basis set augmentations. Nevertheless, the vibrational quantum numbers that characterize these states are retained for augmenting the trial basis. For each mode the highest quantum number associated with a non-negligible FCF (i.e., larger than 10^{-7}) will either increase or

remain the same as in the previous iteration. If the highest quantum number is the same as in the two previous iterations, then convergence has been attained for that particular mode. In that event this maximum quantum number is reduced by two units until a non-negligible FCF is found. The resulting maximum quantum number is marked and kept frozen in subsequent iterations. On the contrary, the nonconverged maximum quantum numbers are increased by one unit in preparation for the next iteration. Because of their symmetry some modes only lead to non-negligible FCF when the value of their associated quantum number is odd or even. That is why in order to consider a progression converged at least the two highest values of their correspondent quantum value must be associated with negligible FCF. An exactly analogous procedure is applied to the minimum quantum numbers except that, again, the minimum value cannot be reduced below zero.

Prior to pruning, the basis set for the next iteration contains all vibrational wave functions within the range of the current maximum and minimum quantum numbers. Then we delete wave functions that were either previously marked for exclusion or characterized by quantum numbers that deviate from those of the reference state by more than the threshold value described above. When the maximum/minimum quantum numbers have converged for all modes, this threshold value is increased by one unit if there is a FCF, for any state at the boundary, that is larger than a preset value (normally 10^{-6}). Finally, the entire calculation is converged when the new basis set is the same as the one used in the previous iteration.

Our procedure for excluding wave functions drastically reduces the growth of the basis set, thereby leading to a major improvement in efficiency. However, it may still happen that the new basis at some iteration is larger than the maximum desirable size. If that occurs, then the new states are split into subsets that are added one at a time without any other basis set augmentations. Ordinarily, subsequent microiterations will remove a sufficient number of states so that all necessary ones can be accommodated.

Our algorithm has been tested in three different ways: (i) the FCF threshold for excluding states was varied from 10^{-5} to 10^{-9}; (ii) the FCF threshold for increasing the range of quantum numbers, when the maximum/minimum values have converged for all modes, was varied from 10^{-4} to 10^{-8}; and (iii) the maximum/minimum quantum number in each cycle was incremented by two and by four rather than by one. Although some of the calculations were far more time consuming than our normal procedure, the differences in the calculated FCFs were always negligible ($<0.1\%$). These tests were run using several different anharmonic PESs for ClO_2.[19]

III. COMPUTATIONAL DETAILS

As an example of the application of our methodology to a polyatomic molecule we have computed FCFs for the $C_2H_4^+\tilde{X}\,^2B_{3u}\leftarrow C_2H_4\tilde{X}\,^1A_g$ ionization band in the He I PE spectrum and the ionization band of the fully deuterated species as well. The *ab initio* electronic structure calculations

TABLE I. Equilibrium geometrical parameters for neutral and cationic ethylene. All quantities are in angstroms and degrees.

| | $C_2H_4 \tilde{X}\,^1A_g$ | | $C_2H_4^+ \tilde{X}\,^2B_{3u}$ | | |
| | D_{2h} | | D_{2h} | D_2 | |
	B3LYP/ 6-311G(d)	Expt.[a]	UB3LYP/ 6-311G(d)	UB3LYP/ 6-311G(d)	Expt.
r(C=C)	1.3271	1.3391	1.4181	1.3952	1.405[b]
r(C–H)	1.0878	1.0868	1.0871	1.0902	1.091[b]
$\angle$(C=C–H)	121.85	121.28	120.84	121.20	121.8[b]
τ(H–C=C–H)	0.00	0.00	0.00	26.92	25[b]/27[c]/29.2[d]

[a]Experimental values from Callomon *et al.* (see Ref. 21).
[b]Derived from a fit to experimental PE spectrum of ethylene by Köppel *et al.* (see Ref. 39).
[c]Derived from a fit to experimental PE spectrum of ethylene by Pollard *et al.* (see Ref. 23).
[d]Derived from a fit to experimental PFI-ZEKE PE spectrum of ethylene by Willitsch *et al.* (see Ref. 25).

were performed at the (U)B3LYP/6-311G(d)[28–30] level. For neutral molecules we used the restricted formalism, while the cationic open shell systems were treated by the unrestricted method which has been shown by Rijkenberg and Buma[31] to give the correct equilibrium torsion angle of 27°. In keeping with the separability of the torsional motion (see later), the harmonic and anharmonic force constants for all other modes were evaluated at the D_{2h}-optimized geometry. Cubic and quartic vibrational force constants were determined by numerical differentiation of quadratic force constants obtained from the GAUSSIAN98 suite of programs.[32] Vibrational displacements of ±0.04 and ±0.08 a.u. were employed for this purpose and the Romberg method[33] was used to reduce numerical error.

Because the torsion potential has a double minimum it is impossible to estimate intensities for the torsional vibration progression based on a zeroth-order harmonic-oscillator model.[34] The FCFs for this progression were, therefore, treated in a special fashion assuming separability of the torsional mode. Thus, the one-dimensional potential-energy function, for both the neutral and the cation, was obtained by *ab initio* calculation at 30 points in the interval from 0° to 60° in the torsion angle. Then, using the program LEVEL 7.4 (Ref. 35) vibrational energies and FCFs were obtained by numerical integration.

The theoretical He I PE spectrum was simulated using Gaussian functions with a full width at half maximum of 20 meV. Relative peak intensities and positions were determined from the theoretical FCFs and vibronic energies. The position of the first peak was shifted, and the intensity scaled, so as to agree with the experimental peak that occurs at the adiabatic ionization energy (AIE) of 10.5122 eV (10.5272 eV) for C_2H_4 (C_2D_4), as measured by Holland *et al.*[24] In our calculations we used the experimental geometry for the neutral molecule and the geometry obtained from an iterative Franck–Condon analysis[5] (IFCA) for the cation. The IFCA procedure involves optimizing the geometrical parameters to obtain the best match between the simulated and experimental spectrum. Chau and co-workers[14–17] have shown that the IFCA geometry of the excited state is the best to use for comparison purposes and that the agreement

between this geometry and that obtained from the highest-level *ab initio* calculations is reasonably good.

IV. RESULTS

Ethylene has a planar D_{2h} equilibrium geometry and the symmetry of the ground state is ^1A_g. Ionization from the $1b_{3u}$ π orbital, which is the highest occupied molecular orbital (HOMO), leads to the $\tilde{X}\,^2B_{3u}$ state of the cation. The equilibrium geometry of this cationic state has D_2 symmetry but, as discussed in the Introduction, the effective symmetry is D_{2h}. *Ab initio* Hartree–Fock calculations yield a planar D_{2h} structure for the cation.[36] Thus, it is necessary to include electron correlation,[31,37] as we do here, in order to obtain a torsional barrier. Table I contains optimized (U)B3LYP/6-311G(d) equilibrium geometry parameters for D_{2h} neutral ethylene, and for the D_{2h} and D_2 cations, as well as the corresponding experimental values. Overall the *ab initio* and experimental values are quite similar; both show the expected increase of the C–C bond length, as well as the loss of planarity, when the π-bonding electron of ethylene is removed. In Table II we present *ab initio* harmonic frequencies for the theoretical equilibrium geometries given in Table I along with some experimental values. The *ab initio* harmonic frequencies are in satisfactory agreement with the available experimental fundamental frequencies. Except for the torsional mode, the difference between the theoretical D_{2h} and D_2 harmonic frequencies of the cation is small in keeping with the separability argument.

The large calculated change in the torsional equilibrium angle and frequency between the D_{2h} and D_2 optimized cation geometries exemplifies the strong anharmonicity of this motion which cannot be treated using the harmonic-oscillator model.[34] On the other hand, the torsional mode is approximately separable from all other normal modes. In fact, the separability is exact at the harmonic level since torsion is the only motion that has a_u symmetry under D_{2h}. Taking anharmonicity into account one expects that the curvilinear angular coordinate will provide a better description of torsion than the corresponding linear normal coordinate.[38] Thus, we assume that the torsional motion is separable when expressed in terms of the torsional angle. In order to obtain vibronic

TABLE II. Theoretical and experimental vibrational frequencies (cm^{-1}) of neutral and cationic ethylene.

Label	Symmetry D_{2h}	Symmetry D_2	$C_2H_4 \widetilde{X}\,^1A_g$ D_{2h} B3LYP/ 6-311G(d)[a]	$C_2H_4 \widetilde{X}\,^1A_g$ D_{2h} Expt.[b]	$C_2H_4^+ \widetilde{X}\,^2B_{3u}$ D_{2h} UB3LP/ 6-311G(d)[a]	$C_2H_4^+ \widetilde{X}\,^2B_{3u}$ D_2 UB3LYP/ 6-311G(d)[a]	$C_2H_4^+ \widetilde{X}\,^2B_{3u}$ D_2 Expt.
ω_1	a_g	a	3137.5	3022	3143.2	3103.0	
ω_2	a_g	a	1699.9	1625	1563.4	1517.9	1510[c]/1487.7[d]
ω_3	a_g	a	1384.9	1344	1272.3	1274.3	1264[c]/1258.7[d]
ω_4	a_u	a	1066.9	1026	453.2i	571.7[e]	83.7[d]
ω_5	b_{1u}	b_1	3122.0	2989	3139.5	3105.8	
ω_6	b_{1u}	b_1	1481.4	1444	1478.6	1441.5	
ω_7	b_{2g}	b_2	955.9	940	1116.1	1075.1	
ω_8	b_{2u}	b_2	3221.3	3105	3264.9	3221.2	
ω_9	b_{2u}	b_2	840.4	826	851.0	804.5	
ω_{10}	b_{3g}	b_3	3192.6	3086	3248.7	3201.8	
ω_{11}	b_{3g}	b_3	1248.5	1222	1244.1	1215.2	
ω_{12}	b_{3u}	b_3	967.1	949	978.6	900.5	901.3[d]

[a]*Ab initio* harmonic frequencies.
[b]Fundamental frequencies from Sension and Hudson (see Ref. 40).
[c]Harmonic frequencies from Pollard *et al.* (see Ref. 23).
[d]Fundamental frequencies from Willitsch *et al.* (see Ref. 25).
[e]Because of the double minimum potential the theoretical harmonic frequency is not expected to be close to the experimental fundamental frequency.

energies and FCFs for this motion, the 1D (U)B3LYP/6-311G(d) potential was computed for both the neutral and cationic molecules as described in Sec. III.

Figure 1 depicts the *ab initio* torsion potential obtained for the cation showing two minima separated by a barrier of 277 cm^{-1}, which is well within the error range of the experimental value given by Pollard *et al.* (270±150 cm^{-1}),[23] and

somewhat lower than the values of 357±26 and 292±24 given by Willitsch *et al.*[25] for $C_2H_4^+$ and $C_2D_4^+$, respectively. Although the difference between the $C_2H_4^+$ and $C_2D_4^+$ barriers obtained by Willitsch *et al.* is not large, it is indicative of anharmonic coupling between torsion and other modes. Our calculated (U)B3LYP/6-311G(d) equilibrium torsion angle of $C_2H_4^+$ reproduces the experimental value ($\sim$28°)
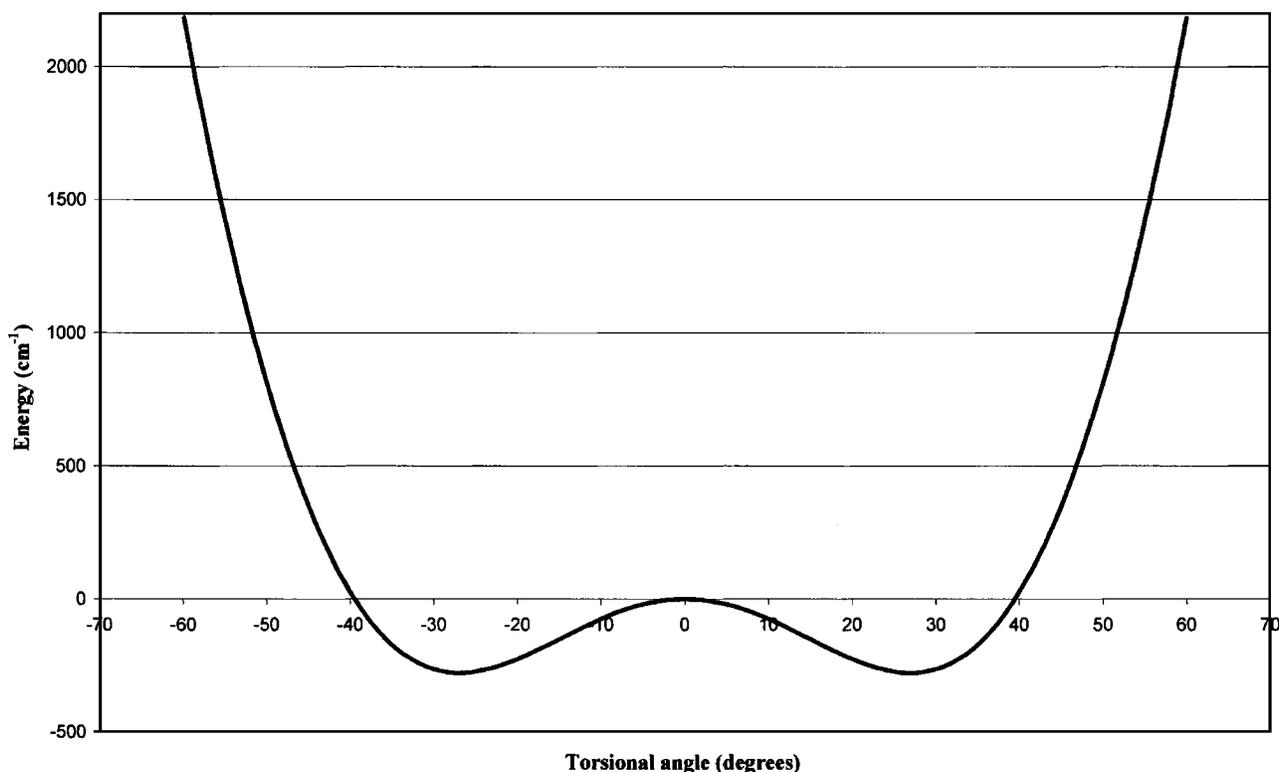

FIG. 1. (U)B3LYP/6-311G(d) torsional potential for $C_2H_4^+ \widetilde{X}\,^2B_{3u}$.

TABLE III. Comparison of calculated (U)B3LYP/6-311G(d) vibrational excitation energies and relative intensities with experiment for even quantum number peaks in the torsion progression for the $^+\tilde{X}\,^2B_{3u} \leftarrow \tilde{X}\,^1A_g$ band of the C_2H_4 and C_2D_4 PE spectra.

	C_2H_4				C_2D_4			
	v_0 (cm^{-1})		Relative intensities		v_0 (cm^{-1})		Relative intensities	
v_4	B3LYP/ 6-311G(d)	Expt.[a]	B3LYP/ 6-311G(d)	Expt.[b]	B3LYP/ 6-311G(d)	Expt.[a]	B3LYP/ 6-311G(d)	Expt.[b]
0	0.0	0.0	100.0	100.0	0.0	0.0	66.8	65.9
2	470.6	438.2	74.9	89.1	285.5	275.4	100.0	100.0
4	1251.2	1162.1	13.4	[c]	767.0	720.7	22.1	20.3

[a]Excitation energies relative to the vibronic ground state observed in the PFI-ZEKE spectra by Willitsch *et al.* (Ref. 25).
[b]Peak heights without correction for overlapping structures measured by Holland *et al.* (see Ref. 24).
[c]Not observed because it is overlapped by another peak.

(Refs. 23 and 25) quite well. Relative intensities for the even quantum number peaks in the torsional progression, obtained from the FCFs determined by numerical integration using LEVEL 7.4,[35] are given in Table III along with the vibronic energies. The errors compared to experiment are fairly small considering that we have ignored anharmonic coupling with the remaining modes and have done no empirical fitting, which is often the case in other treatments.[13–17,19,25] Note that our calculation successfully reproduces the fact that deuteration causes a shift in the most intense peak from $v=0$ to $v=2$. In the concluding section we will discuss future plans to incorporate the anharmonic coupling between torsion and other modes.

The FCFs are very sensitive to the geometry of the neutral and cation. Like Chau and co-workers[14–17] we have used the experimental geometry of neutral ethylene[21] together with the IFCA (Ref. 5) geometry of the cation in simulating spectra for the other $3N$-7 normal modes. Besides the torsion mode (ω_4), only the a_g symmetry C=C stretch (ω_2) and CH$_2$ scissors bend (ω_3) modes are involved in the progressions observed in the experimental PE spectra of Pollard *et al.*[23] and Holland *et al.*[24] Thus, in our simulations we optimized the C=C bond length and CH$_2$ angle of the (effective) D_{2h} cation using the IFCA method, and kept the (U)B3LYP/6-311G(d) value of the C–H bond length. Table IV gives IFCA values of these geometric parameters for $C_2H_4^+$ and $C_2D_4^+$ obtained by computing FCFs at the harmonic, first-order perturbation-theory (PT1), and second-order perturbation-theory (PT2) levels. The IFCA results can be considered valid only if they are not very different from the *ab initio* equilibrium parameters.[13–16] This is the case

here as can readily be seen from a comparison of Tables I and IV.

In Figs. 2 and 3 we contrast the harmonic (Fig. 2) and PT1 (Fig. 3) simulated first band of the C_2H_4 He I PE spectrum with the PT2 simulation; while in Table V we give theoretical frequencies and FCFs for the individual peaks evaluated at the PT2 level. Except for the 1D torsional progression, all FCFs were calculated with our new procedure.[19] The efficiency of our algorithm is such that the PT2 simulation can be run on a personal laptop computer in less than an hour. Figure 2 shows that the main effect of anharmonicity, as far as FCFs are concerned, is to reduce the relative intensity of the low-frequency peaks while incrementing the relative intensity of the high-frequency peaks. Anharmonicity also decreases the frequency of all the peaks, with the reduction being larger on the high-frequency side of the spectrum. The reader may view the peak $(v_1 v_2 v_3 v_4) = (0120)$ as a good example showing the effect of anharmonicity on the FCFs and frequencies. Although the PT1 frequencies are unaltered from the harmonic ones, as mentioned previously, one can see from the comparison with PT2 in Fig. 3 that the effect of anharmonicity on the FCFs is mostly incorporated at the PT1 level. This result may be useful because the PT2 calculation for ethylene takes four times as much CPU time as the PT1 calculation. We note here that our previous results for ClO_2 (Ref. 19) also showed a good performance of PT1 for the FCFs.

In constructing the vibrational basis set all modes other than torsion were considered. However, only the a_g C=C stretch and CH$_2$ scissors bend modes are associated with non-negligible FCFs. For comparison purposes, then, we re-

TABLE IV. C=C bond lengths and C=C–H angles obtained for D_{2h} $C_2H_4^+$, and $C_2D_4^+$ using the IFCA procedure with FCFs computed at the harmonic, PT1, and PT2 levels. All quantities are in angstroms and degrees.

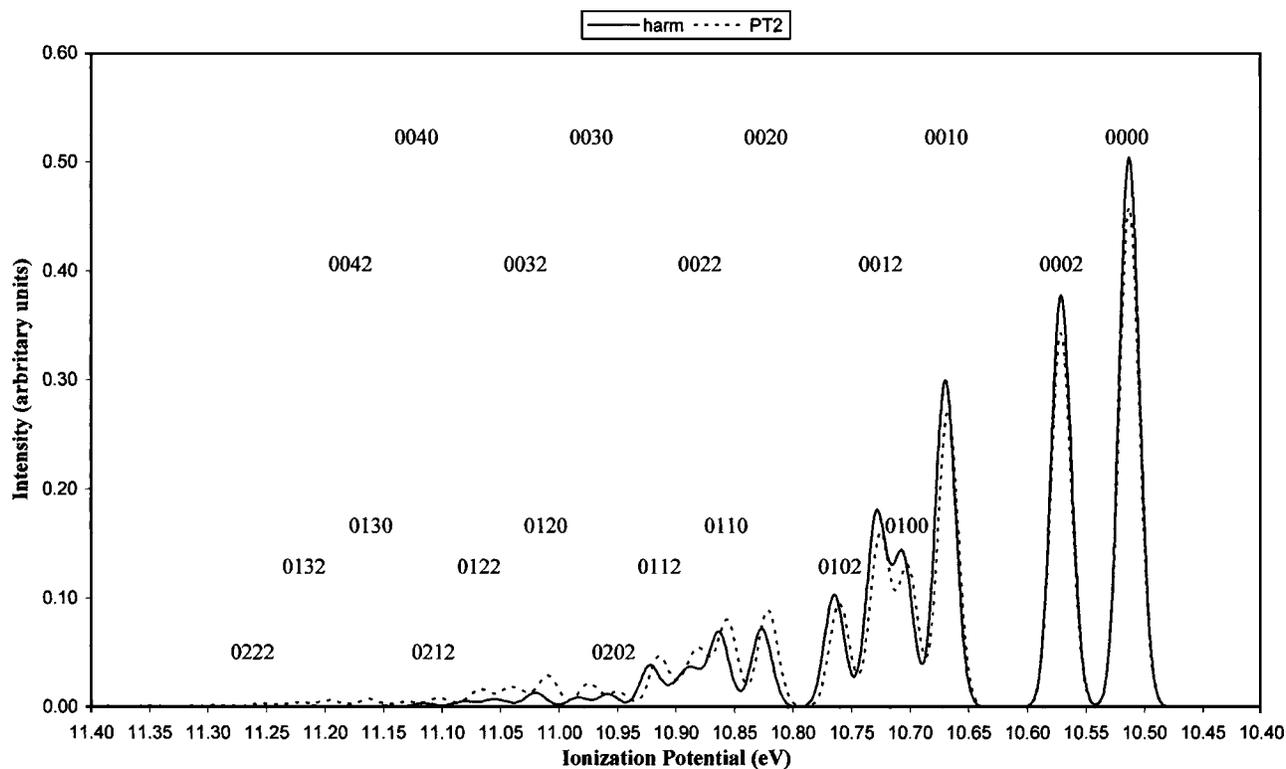|	$C_2H_4^+$			$C_2D_4^+$		
	Harmonic	PT1	PT2	Harmonic	PT1	PT2
r(C=C)	1.4093	1.4122	1.4135	1.4055	1.4080	1.4072
$\angle$(C=C–H)	119.90	119.83	119.70	120.74	120.68	120.75

FIG. 2. (U)B3LYP/6-311G(d) simulation of the first band in the C_2H_4 He I PE spectrum. The solid and dashed lines represent the harmonic and PT2 anharmonic spectra, respectively.
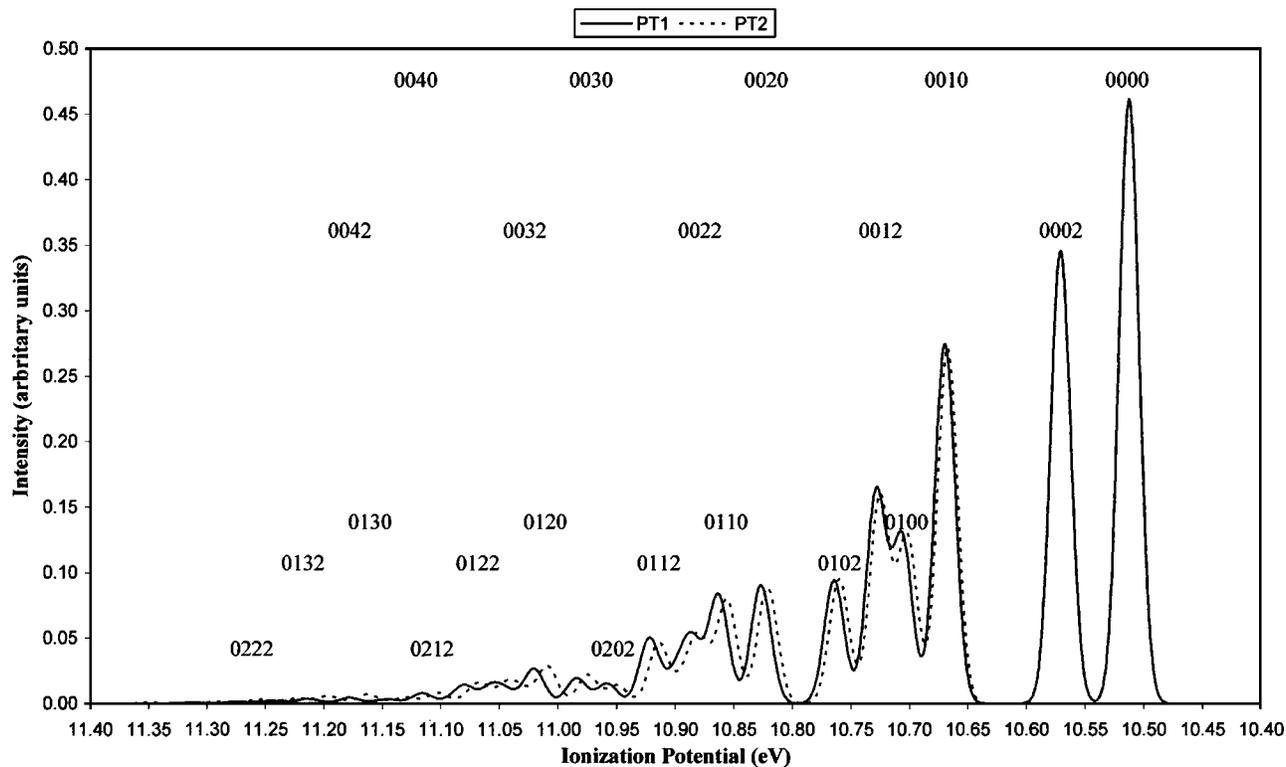

FIG. 3. (U)B3LYP/6-311G(d) simulation of the first band in the C_2H_4 He I PE spectrum. The solid and dashed lines represent the PT1 and PT2 anharmonic spectra, respectively.

TABLE V. (U)B3LYP/6-311G(d) frequencies and FCFs for the $^+\widetilde{X}\,^2B_{3u}$ $\leftarrow\widetilde{X}\,^1A_g$ band of the C_2H_4 PE spectrum computed at the PT2 level. The FCFs are in arbitrary units.

$v_1v_2v_3v_4$	Freq. (eV)	FCF	$v_1v_2v_3v_4$	Freq. (eV)	FCF
0000	10.51	4.53×10^{-1}	0032	11.04	1.07×10^{-2}
0002	10.57	3.39×10^{-1}	0204	11.04	2.41×10^{-3}
0010	10.67	2.09×10^{-1}	0210	11.04	1.09×10^{-2}
0004	10.67	6.08×10^{-2}	0122	11.07	1.56×10^{-2}
0100	10.70	1.27×10^{-1}	0300	11.08	2.05×10^{-3}
0012	10.72	1.56×10^{-1}	0212	11.10	8.17×10^{-3}
0102	10.76	9.49×10^{-2}	0040	11.13	2.25×10^{-3}
0014	10.82	2.80×10^{-2}	0034	11.13	1.91×10^{-3}
0020	10.82	6.05×10^{-2}	0302	11.14	1.54×10^{-3}
0104	10.85	1.70×10^{-2}	0130	11.16	4.75×10^{-3}
0110	10.86	6.19×10^{-2}	0124	11.17	2.79×10^{-3}
0022	10.88	4.53×10^{-2}	0042	11.19	1.68×10^{-3}
0200	10.89	1.79×10^{-2}	0220	11.20	3.93×10^{-3}
0112	10.91	4.64×10^{-2}	0214	11.20	1.46×10^{-3}
0202	10.95	1.34×10^{-2}	0132	11.22	3.55×10^{-3}
0030	10.98	1.42×10^{-2}	0310	11.23	1.50×10^{-3}
0024	10.98	8.11×10^{-3}	0222	11.26	2.94×10^{-3}
0114	11.01	8.30×10^{-3}	0312	11.29	1.12×10^{-3}
0120	11.01	2.08×10^{-2}			

peated the simulation including only these two normal modes in the basis set. The difference between the two simulations is negligible. However, the difference in CPU time is dramatic; the PT2 calculation using two modes requires less than a second of personal laptop computer CPU time. In addition, the PES part of the calculation is faster by a factor of 5.

In Figs. 4 and 5 we separately compare our harmonic (Fig. 4) and PT2 (Fig. 5) simulations with the experimental C_2H_4 spectrum obtained by Holland et al.[24] Since the experimental intensities are in arbitrary units, we forced the intensity of the experimental (0000) peak to equal the theoretical value. At this point we remind the reader that the simulation of the torsional progression is purely ab initio. It has not been adjusted using the IFCA procedure and anharmonic coupling between torsion and other modes has been neglected. That is why the agreement between the theoretical and experimental intensities is poorer for the $(0v_2v_32)$ peaks than for the others. There are five progressions labeled in the experimental spectra. They are all associated either with the C=C stretch, CH_2 scissors bend, or torsion mode. These same progressions can be clearly seen in our theoretical simulations. Other progressions are present but they cannot be observed separately because they are overlapped by the most intense ones. For example, the progression (0004), (0014), (0024), and (0034) is overlapped by (0010), (0020), (0030), and (0040). Nonetheless, the latter contributes from 22% to 46% of the total intensity for each peak. Similarly, (0104), (0114), and (0124) are overlapped by (0110), (0120), and (0130). Again the less important progression provides more than a fifth of each peak intensity.

By comparing Figs. 4 and 5 we see that anharmonicity is essential to reproduce experiment for nonfundamental excitations such as (0020), (0110), (0030), or (0120). The need for the IFCA procedure, and the remaining lack of agreement between the PT2 and experimental spectra, is due to some combination of (i) anharmonicity contributions higher than second order, (ii) intrinsic limitations of perturbation theory,
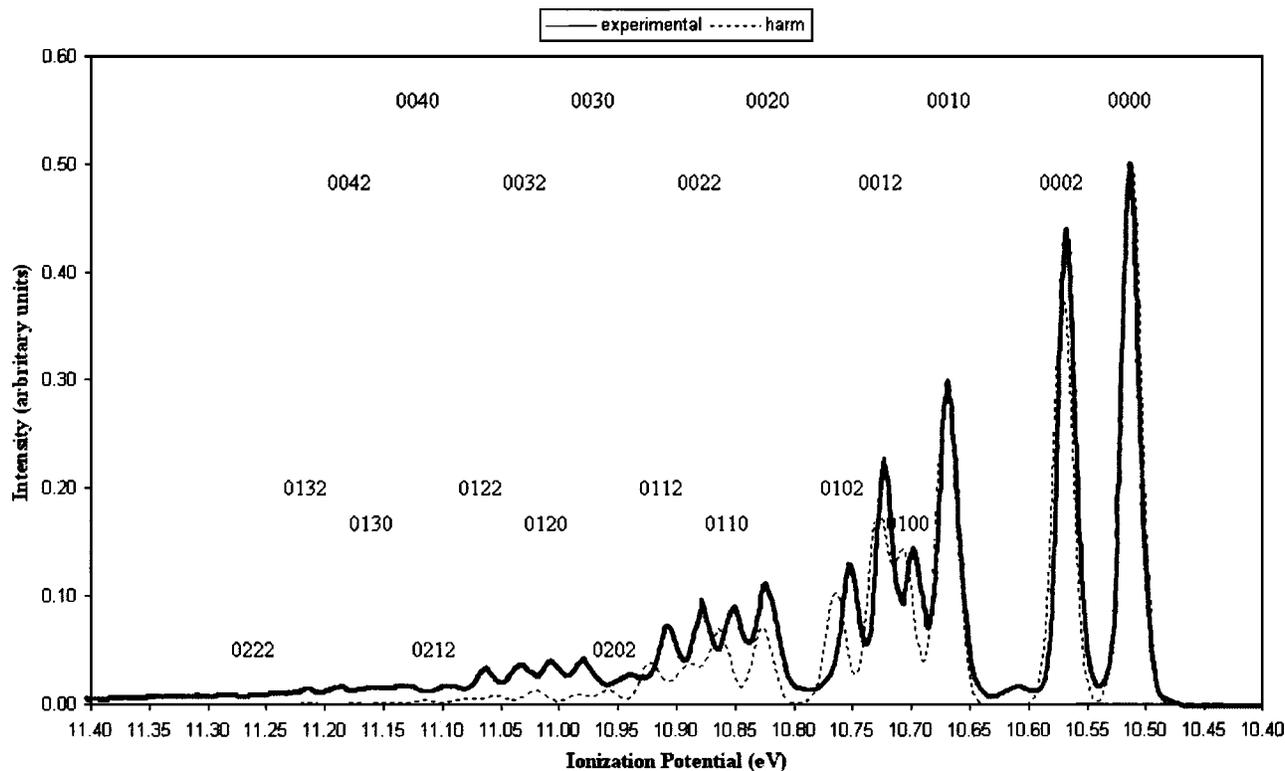

FIG. 4. Experimental results obtained by Holland et al. (see Ref. 24) (solid line) and (U)B3LYP/6-311G(d) harmonic level simulation (dashed line) for the first band in the C_2H_4 He I PE spectrum.
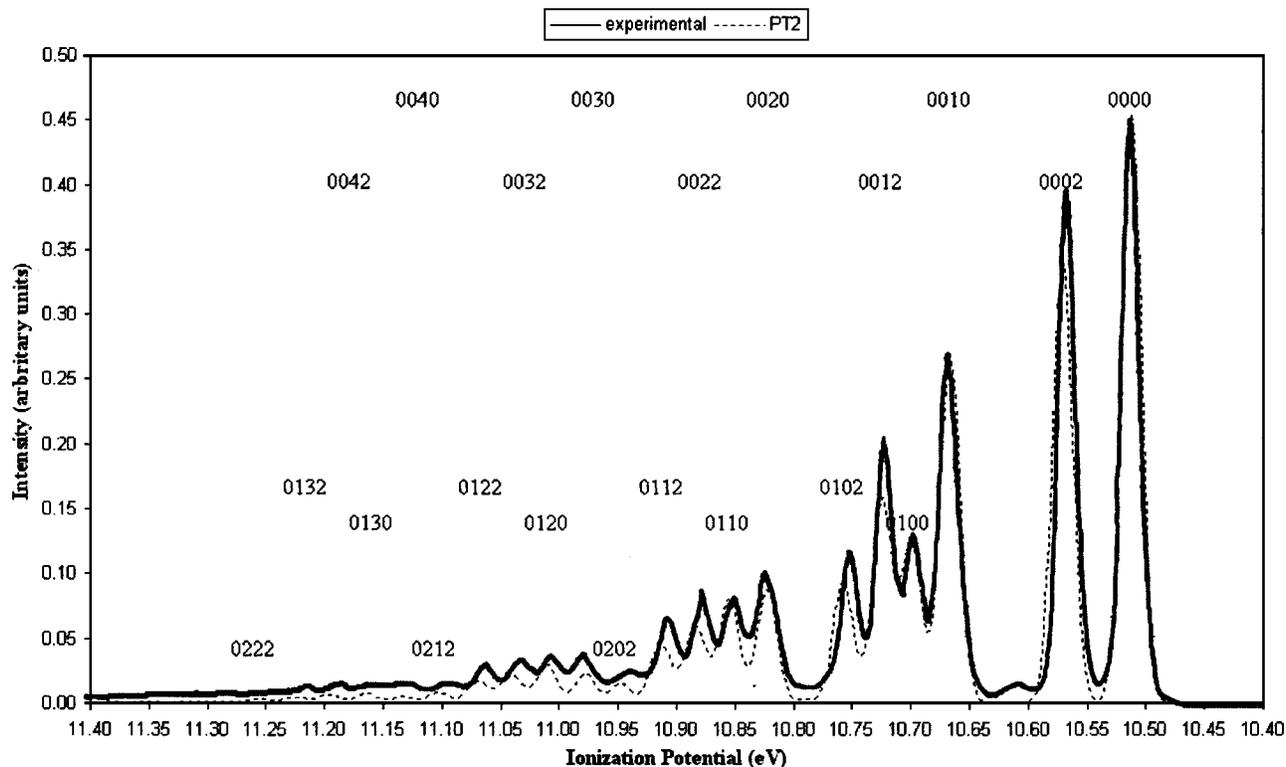
FIG. 5. Experimental results by Holland *et al.* (see Ref. 24) (solid line) and (U)B3LYP/6-311G(d) PT2 level simulation (dashed line) for the first band in the C_2H_4 He I PE spectrum.
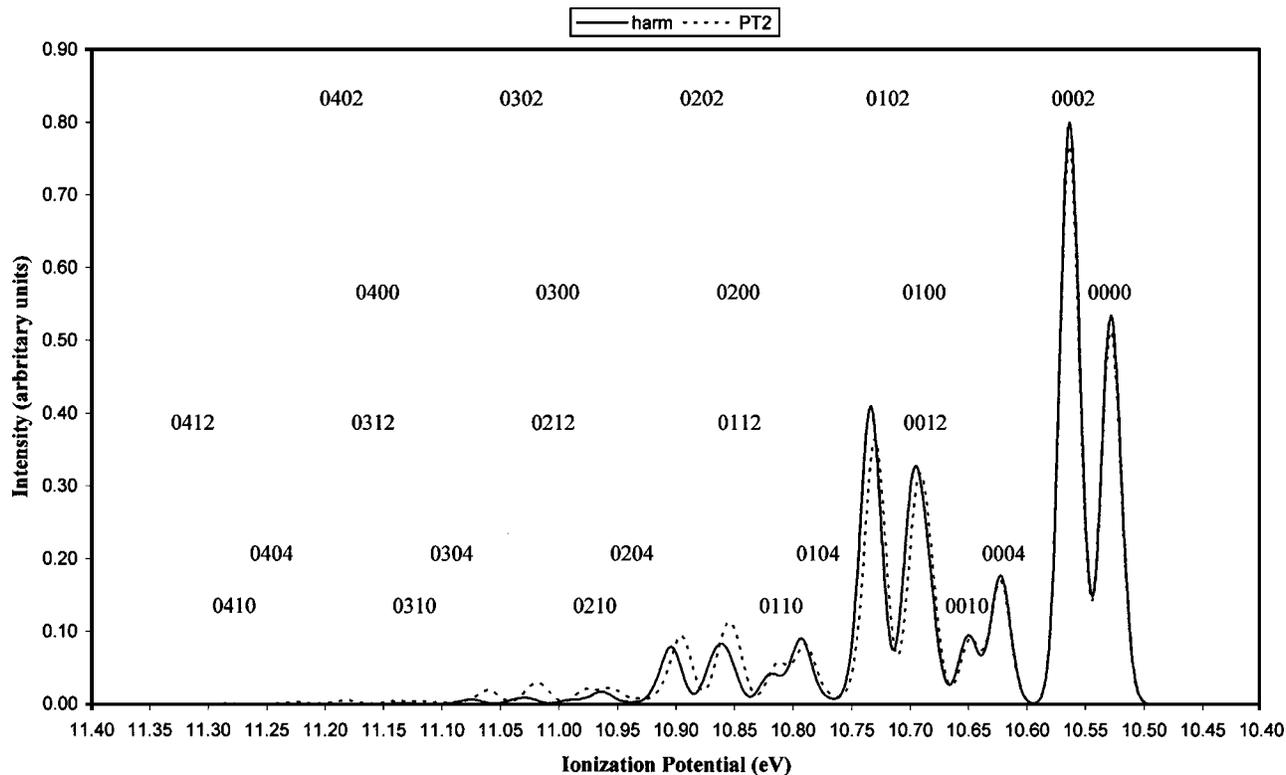

FIG. 6. (U)B3LYP/6-311G(d) simulation of the first band in the C_2D_4 He I PE spectrum. The solid and dashed lines represent the harmonic level and PT2 anharmonic level treatments, respectively.

TABLE VI. (U)B3LYP/6-311G(d) frequencies and FCFs for the $^{+}\tilde{X}\,^{2}B_{3u}$ $\leftarrow \tilde{X}\,^{1}A_{g}$ band of the C_2D_4 PE spectrum computed at the PT2 level. The FCFs are in arbitrary units.

$v_1v_2v_3v_4$	Freq. (eV)	FCF	$v_1v_2v_3v_4$	Freq. (eV)	FCF
0000	10.53	5.13×10^{-1}	0032	10.93	1.48×10^{-3}
0002	10.56	7.69×10^{-1}	0120	10.93	6.09×10^{-3}
0004	10.62	1.70×10^{-1}	0204	10.95	1.99×10^{-2}
0010	10.65	8.95×10^{-2}	0122	10.97	9.12×10^{-3}
0012	10.68	1.34×10^{-1}	0210	10.98	1.40×10^{-2}
0100	10.69	2.39×10^{-1}	0212	11.01	2.10×10^{-2}
0102	10.73	3.57×10^{-1}	0300	11.02	1.23×10^{-2}
0014	10.74	2.96×10^{-2}	0124	11.03	2.01×10^{-3}
0020	10.77	1.04×10^{-2}	0302	11.06	1.83×10^{-2}
0100	10.79	7.89×10^{-2}	0214	11.07	4.64×10^{-3}
0022	10.80	1.55×10^{-2}	0220	11.10	1.68×10^{-3}
0110	10.81	4.74×10^{-2}	0304	11.12	4.05×10^{-3}
0112	10.85	7.10×10^{-2}	0222	11.14	2.51×10^{-3}
0200	10.86	6.02×10^{-2}	0310	11.14	2.65×10^{-3}
0024	10.86	3.43×10^{-3}	0312	11.18	3.96×10^{-3}
0202	10.89	9.01×10^{-2}	0400	11.19	1.75×10^{-3}
0114	10.91	1.57×10^{-2}	0402	11.22	2.62×10^{-3}

and (iii) nonseparability of the torsional mode. In the Sec. V we will discuss future plans to remove these deficiencies.

In Fig. 6 we present the harmonic and PT2 simulations of the first band in the C_2D_4 He I PE spectrum. The PT2 frequencies and FCFs are given in Table VI. Deuteration of ethylene leads to a major change in the shape of the spectrum. In the case of C_2D_4 the absolute intensity of the torsional progressions increases and, in addition, the ω_2 progressions become more intense than those of ω_3. There are, again, significant differences between the harmonic and PT2 spectra with regard to intensity and frequency. Once more, introduction of anharmonicity reduces the FCFs for low-energy peaks and increases the intensity of the high-energy peaks.

In Fig. 7 we compare our theoretical PT2 spectra for C_2D_4 with the experimental results obtained by Holland et al.[24] Again, all progressions labeled in the experimental spectra are clearly observed in the simulations. However, there are important aspects revealed by theory that are not evident from experiment. For example, in the progression labeled $(0v_212)$ the dominant contribution to the intensity of (0012) actually arises from the overlapping (0100) peak. Furthermore, progressions such as $(0v_214)$, $(0v_220)$, and $(0v_222)$ do not explicitly appear in the experimental spectrum because they are overlapped rather than weak in intensity. As in the case of C_2H_4, there is essentially no difference between the spectra predicted using only the a_g C=C stretch and CH_2 scissors bend modes in the basis set rather than all (except for torsion) $3N$-7 modes. From Figs. 6 and 7 it is also evident, as for C_2H_4, that the PT2 spectrum represents a definite improvement over the harmonic level treatment. The peak (0200) well illustrates this point with regard to both the intensity and frequency.

In comparing C_2H_4 with C_2D_4, it is important to note that our best results are noticeably poorer for the deuterated species because of the more prominent role of the torsional progressions in the latter case. One clear example is given by the comparison of intensity ratios between (0002)/(0000)
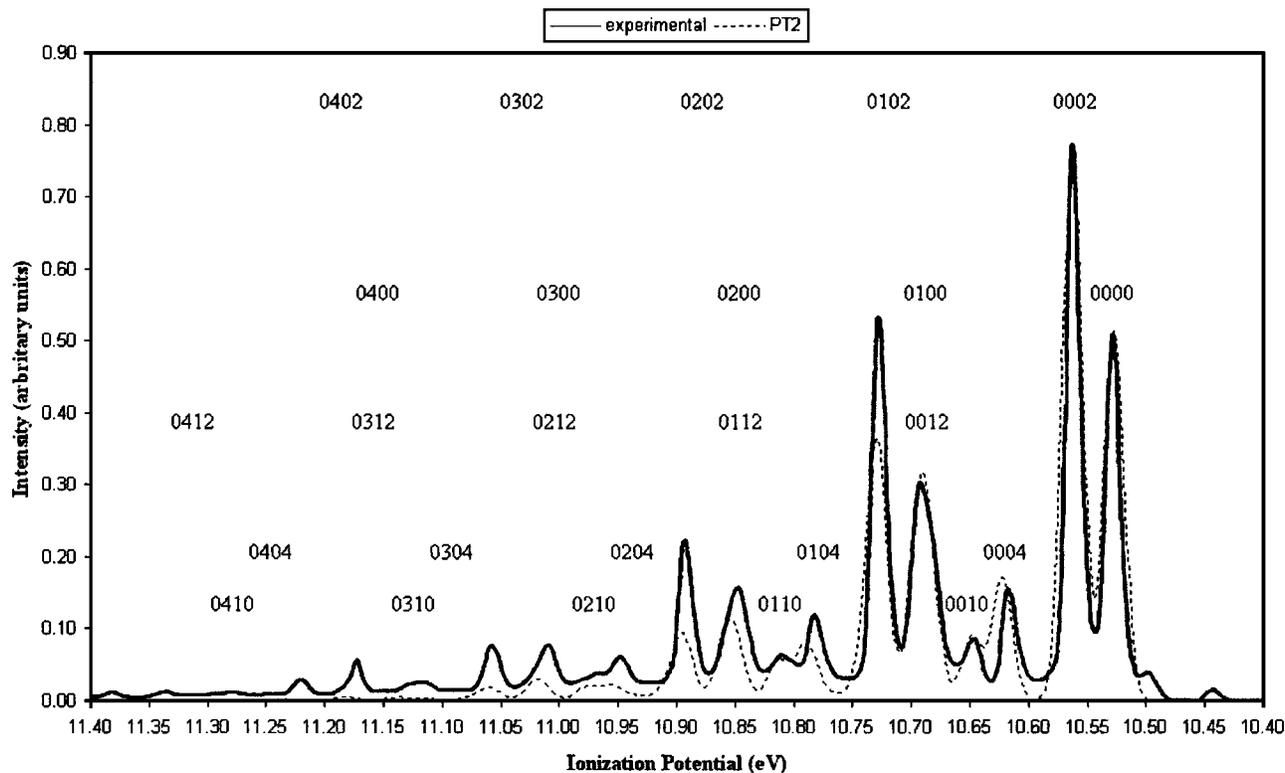

FIG. 7. Experimental results obtained by Holland et al. (see Ref. 24) (solid line) and (U)B3LYP/6-311G(d) simulation at the PT2 level (dashed line) for the first band in the C_2D_4 He I PE spectrum.

and $(0102)/(0100)$. Whereas the theoretical simulation for C_2D_4 reproduces the first ratio very well, the result for the second ratio is not nearly as good. This makes it appear that the nonseparability of the torsional mode may be the main source of disagreement between the theoretical and experimental spectra.

V. CONCLUSIONS

The simple procedure we have recently presented for calculating Franck–Condon factors (FCFs) has been used to characterize the $C_2H_4^+\tilde{X}\,^2B_{3u}\leftarrow C_2H_4\tilde{X}\,^1A_g$ band in the photoelectron spectrum. Unlike other treatments, this procedure includes nondiagonal anharmonic coupling (i.e., mode-mode coupling) as well as diagonal anharmonicity terms and Duschinsky rotations. Anharmonic effects are incorporated by means of perturbation theory. A new and improved algorithm is given for generating a minimal basis set of vibrational states that must be taken into account in solving the coupled simultaneous equations for the FCFs. As a result the calculation of a spectrum at the PT2 level takes less than 1 h on a personal laptop computer. The computer time is reduced to less than 1 s, without loss of accuracy, by eliminating all states from the vibrational basis other than those corresponding to excitations of the $C=C$ stretch, the CH_2 scissors bend, and the torsion. The torsional motion, which leads to a twisted D_2 geometry in the cationic state, is treated in a unique manner because it is so highly anharmonic. We assume that motion involving the torsion angle is separable from other modes so that the diagonal anharmonicity can be treated exactly. Good agreement with experiment is then obtained for both C_2H_4 and C_2D_4 using second-order perturbation theory for the remaining modes. These perturbation corrections are significant. A first-order treatment suffices for the FCFs but not for the frequencies. Our results for C_2D_4, while satisfactory, are not as good as those for C_2H_4 because the torsional progressions are more prominent in the former case and separability has been assumed.

Although the present method does give satisfactory results, there is room for improvement. In the future we plan to replace the perturbation treatment with a variational approach, just as we have very recently done for vibrational (hyper)polarizabilities.[41] Large anharmonicity terms are difficult to treat using perturbation theory, but they can be successfully dealt with by applying the variational methods of electron structure theory to the vibrational Schrödinger equation. The basic equation of this paper, namely, Eq. (5), may be reformulated so that the variational approach can be employed to calculate FCFs. That will allow us to include anharmonic contributions higher than second order and to remove the intrinsic limitations of the perturbation expansion in terms of normal coordinates. Even at the lowest level of variation treatment, i.e., the vibrational self-consistent field (VSCF) method, the most important off-diagonal anharmonic coupling with torsion is incorporated along with the full 1D torsional potential.

ACKNOWLEDGMENTS

[1] J. Franck, Trans. Faraday Soc. **21**, 536 (1925).

[2] E. U. Condon, Phys. Rev. **32**, 858 (1928).

[3] G. Herzberg and E. Teller, Z. Phys. Chem. Abt. B **21**, 410 (1933).

[4] T. E. Sharp and H. M. Rosenstock, J. Chem. Phys. **41**, 3453 (1964).

[5] P. Chen, in *Unimolecular and Bimolecular Ion-Molecule Reaction Dynamics*, edited by C.-Y. Ng, T. Baer, and I. Powis (Wiley, Chichester, 1994), p. 371.

[6] K. M. Ervin, T. M. Ramond, G. E. Davico, R. L. Schwartz, S. M. Casey, and W. C. Lineberger, J. Phys. Chem. A **105**, 10822 (2001).

[7] H. Kikuchi, M. Kubo, N. Watanabe, and H. Suzuki, J. Chem. Phys. **119**, 729 (2003).

[8] E. V. Doctorov, I. A. Malkin, and V. I. Man'ko, J. Mol. Spectrosc. **64**, 302 (1977).

[9] B. Segev and E. J. Heller, J. Chem. Phys. **112**, 4004 (2000).

[10] S. Kallush, B. Segev, A. V. Sergeev, and E. J. Heller, J. Phys. Chem. A **106**, 6006 (2002).

[11] F. Iachello and S. Oss, Phys. Rev. Lett. **66**, 2976 (1991).

[12] H. Ishikawa, H. Toyosaki, N. Mikani, F. Pérez-Bernal, P. H. Vaccaro, and F. Iachello, Chem. Phys. Lett. **365**, 57 (2002).

[13] D. K. W. Mok, E. P. F. Lee, F.-T. Chau, D. Wang, and J. M. Dyke, J. Chem. Phys. **113**, 5791 (2000).

[14] E. P. F. Lee, D. K. W. Mok, F.-T. Chau, and J. M. Dyke, J. Chem. Phys. **121**, 2962 (2004).

[15] F.-T. Chau, D. K. W. Mok, E. P. F. Lee, and J. M. Dyke, J. Chem. Phys. **121**, 1810 (2004).

[16] N. Bulcourt, J.-P. Booth, E. A. Hudson, J. Luque, D. K. W. Mok, E. P. Lee, F.-T. Chau, and J. M. Dyke, J. Chem. Phys. **120**, 9499 (2004).

[17] D. K. W. Mok, E. P. F. Lee, F.-T. Chau, and J. M. Dyke, J. Chem. Phys. **120**, 1292 (2004).

[18] A. Hazra, H. H. Chang, and M. Nooijen, J. Chem. Phys. **121**, 2125 (2004).

[19] J. M. Luis, D. M. Bishop, and B. Kirtman, J. Chem. Phys. **120**, 813 (2004).

[20] F. Duschinsky, Acta Physicochim. URSS **7**, 551 (1937).

[21] J. H. Callomon, E. Hirota, T. Iijima, K. Kuchitsu, and W. J. Lafferty, in *Structure Data of Free Polyatomic Molecules*, Landolt-Börnstein New Series II Vol. 15, edited by K.-H. Hellwege and A. M. Hellwege (Springer, Berlin, 1987), p. 608.

[22] A. J. Merer and L. Schoonveld, Can. J. Phys. **47**, 1371 (1969).

[23] J. E. Pollard, D. J. Trevor, J. E. Reutt, Y. T. Lee, and D. A. Shirley, J. Chem. Phys. **81**, 5302 (1984).

[24] D. M. P. Holland, D. A. Shaw, M. A. Hayes, L. G. Shpinkova, E. E. Rennie, L. Karlsson, P. Baltzer, and B. Wannberg, Chem. Phys. **219**, 91 (1997).

[25] S. Willitsch, U. Hollenstein, and F. Merkt, J. Chem. Phys. **120**, 1761 (2004).

[26] E. B. Wilson, Jr., J. C. Decius, and P. C. Cross, in *Molecular Vibrations, The Theory of Infrared and Raman Vibrational Spectra* (Dover Publications, Inc., New York, 1955).

[27] J. O. Hirschfelder, W. Byers Brown, and S. T. Epstein, Adv. Quantum Chem. **1**, 255 (1964).

[28] A. D. Becke, J. Chem. Phys. **98**, 5648 (1993).

[29] C. Lee, W. Yang, and R. G. Parr, Phys. Rev. B **37**, 785 (1988).

[30] P. C. Hariharan and J. A. Pople, Theor. Chim. Acta **28**, 213 (1973).

[31] R. A. Rijkenberg and W. J. Buma, J. Phys. Chem. A **106**, 3727 (2002).

[32] M. J. Frisch, G. W. Trucks, H. B. Schlegel *et al.*, GAUSSIAN 98, Revision A.11, Gaussian, Inc., Pittsburgh, PA, 2001.

[33] P. J. Davis and P. Rabinowitz, in *Numerical Integration* (Blaisdell, London, 1967), p. 166.

[34] K. Takeshita, J. Chem. Phys. **95**, 1838 (1991).

[35] R. J. Le Roy, Chemical Physics Research Report CP-642 R^3 (University of Waterloo, Ontario, 2001).

[36] K. Somasundram and N. C. Handy, J. Chem. Phys. **84**, 2899 (1986).

[37] M. L. Abrams, E. F. Valeev, C. D. Sherrill, and T. D. Crawford, J. Phys. Chem. A **106**, 2671 (2002).

[38] J. R. Reimers, J. Chem. Phys. **115**, 9103 (2001).

[39] H. Köppel, W. Domcke, L. S. Cederbaum, and W. von Niessen, J. Chem. Phys. **69**, 4252 (1978).

[40] R. J. Sension and B. S. Hudson, J. Chem. Phys. **90**, 1377 (1989).

[41] M. Torrent-Sucarrat, J. M. Luis, and B. Kirtman, J. Chem. Phys. (accepted).